AMS ^{14}C DATING AND STABLE ISOTOPE ANALYSIS ON AN 8-KYR OYSTER SHELL FROM TAIPEI BASIN: SEA LEVEL AND SST CHANGES

Hong-Chun Li[1,3]* • Horng-Sheng Mii[2] • Tsung-Kwei Liu[1] • Wen-Shan Chen[1] • Su-Chen Kang[1] • Chun-Yen Chou[1] • Satabdi Misra[1] • Tzu-Tsen Shen[1] • Meixun Zhao[3]

[1]Department of Geosciences, National Taiwan University, Taipei 10617, Taiwan, ROC
[2]Department of Earth Sciences, National Taiwan Normal University, Taipei 11677, Taiwan, ROC
[3]Frontiers Science Center for Deep Ocean Multispheres and Earth System, and Key Laboratory of Marine Chemistry Theory and Technology, Ministry of Education, Ocean University of China, Qingdao, China

ABSTRACT. Seven accelerator mass spectrometry radiocarbon (AMS ^{14}C) dates (7260±106~7607±95 BP averaged 7444 ±103 BP) on a giant oyster shell, collected from an ancient shore of the Taipei Basin, are similar to the LSC (liquid scintillation counting) ^{14}C age (7260±46 BP) of a grass sample inside the shell. The calibrated ^{14}C ages of the C. *gigas* by Marine20 are 7490±240~7805±230 cal BP (average 7660±96 cal BP), generally agreed with the calibrated LSC ^{14}C ages of the grass and the oyster shell. Combined with other ^{14}C ages of shoreline samples in the Taipei Basin, it is evident that sea level rose from 8600 to 7600 cal BP and reached a stand higher than modern sea level. During this marine transgression, the sedimentation rate along the shoreline was very high because ^{14}C dating was not able to detect age differences for 4–5 m thick sediment sequences. Sixty-nine analyses of $\delta^{18}O$ and $\delta^{13}C$ from the oldest part of the shell exhibit clear seasonal cycles, with a 4-year period of growth in the 5.5-cm section. According to the $\delta^{18}O$ values, the ancient oyster grew in a warmer-than-present shoreline environment, suggesting that the current absence of the giant oyster in Taiwan is not due to warming conditions.

KEYWORDS: [14]C dating, early-mid Holocene, oyster shell, stable isotopes, Taipei Basin.

1. INTRODUCTION

The Taipei metropolitan area or Greater Taipei area is the largest metropolitan area in Taiwan with an elevation of fewer than 20 m and located only 10 km away from the ocean (with current sea level; Figure 1). Previous studies have shown that about 670 m of Quaternary sediments in the Taipei Basin revealed multiple marine transgressions which turned the area to a large brackish body of water (e.g., Liew et al. 1997; Teng et al. 2000). The last invasion of ocean water into the basin in response to sea level rise was in the early Holocene (Chen et al. 2008; Su et al. 2018). Su et al. (2018) documented that seawater encroached into the Taipei Basin from the Tamsui River about 10,000 years ago and reached its maximum around 8000 years ago based on 66 ^{14}C dates from 23 drill cores over Taipei Basin. The sea level retreated around 6000 years ago. However, owing to the sample limitation, the duration and maximum area of the marine transgression in the basin are not well known. Under the current global warming, concerns about the impact of rising sea levels on Taipei Basin become an important issue. Any information about the ancient seawater intrusion (e.g., when, how long and how big?) will help us in understanding and modelling of future events.

In the present study, a giant oyster shell (42 cm long), *Crassostrea gigas* (hereafter *C. gigas*), was uncovered from an oyster reef on the ancient shore of eastern Taipei Basin in 2002 during construction work (Figure 1). The sampling section provides good evidence of the seawater transgression in Taipei Basin. This study aims to determine the following: (1) the time duration of the marine deposits, (2) the sea level represented by the studying section, and (3) the climatic condition during the time of deposition. Additionally, oyster species of such large size have not appeared around Taiwan since the late Holocene, but native *C. gigas* can be found in cold latitudes

---

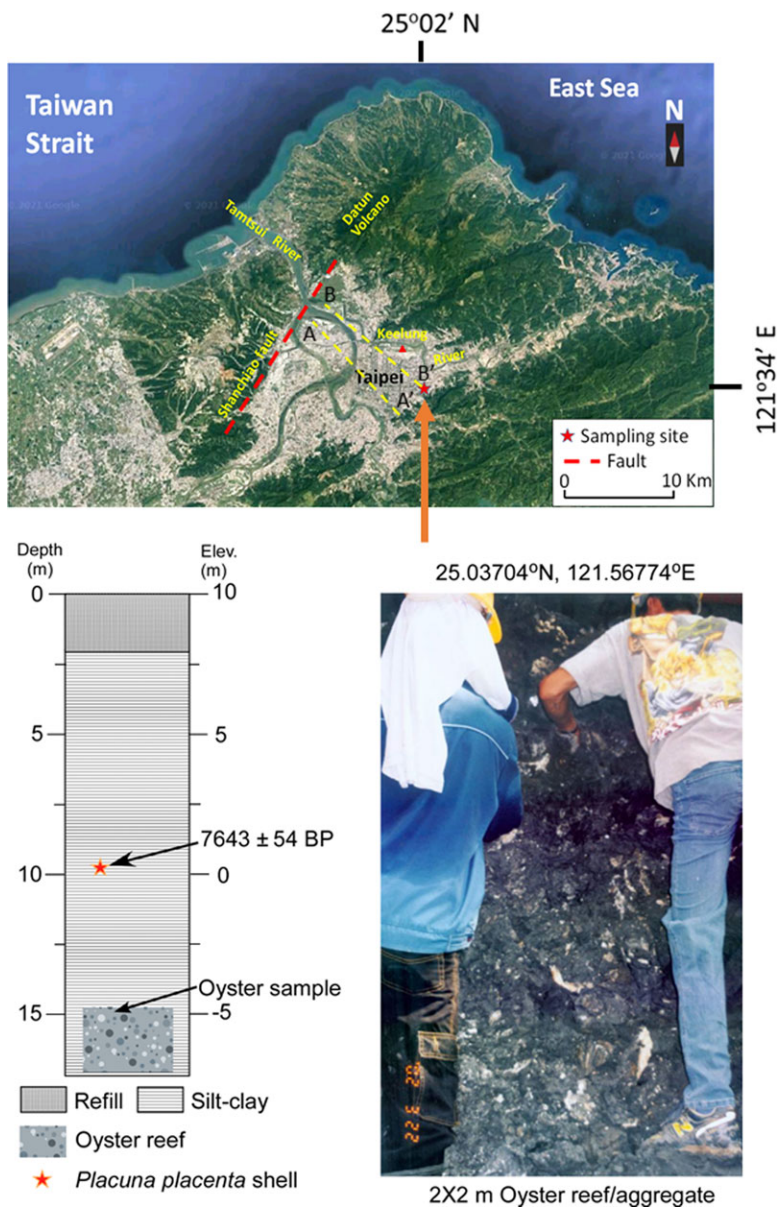*Corresponding author. Email: hcli1960@ntu.edu.tw

Figure 1   Map of Taipei Basin and sampling location. Taipei Basin is shown on the upper panel map. The red broken line denotes Shanchiao normal fault. Two dashed lines with A-A' and B-B' indicate the transects of drill cores in the basin. The red star and red triangle denote the sites of all samples in Table 1. In the lower panel, a sketch figure on the left side describes the sample section, and the oyster reef is shown on the right side picture. The oyster reef is 14 m below the ground surface (–5 m current sea level). A *Placuna placenta* (hereafter *P. placenta*) shell collected 5 m above the oyster reef was dated, resulting 7643±54 BP. (Please see online version for color figures.)

such as Japan, Korea and N. China (Escapa et al. 2004; Miossec et al. 2009). Considering the oyster species currently lives in cooler seawater, was the water temperature cooler during a high stand of sea level when the giant oyster existed in the Taipei Basin? Therefore, one hypothesis regarding the extinction of giant oyster in Taiwan was attributable to the temperature variation.

It is well known that the ^{14}C ages of marine carbonate deposits need to be calibrated by marine calibration curve for the marine reservoir effect (e.g., Marine20 by Heaton et al. 2020). Previous studies have shown that marine reservoir effects do exist in intertidal zones, but only pre-bomb shells are used to estimate marine reservoir effects (Alves et al. 2018; Hadden et al. 2023; O'Connor et al. 2010; Yang et al. 2019; Yoneda et al. 2007). Chen et al. (2020) used a large number of ^{14}C dates on samples including marine shells, boring shells, charcoals and corals to determine the ages of marine terraces along the east coastal range of Taiwan. They calibrated the ages of marine shells with Marine20 and $\Delta R = 101\pm49$ years. Radiocarbon dating on the marine shells of the current study will provide a cross-check for calibration of marine reservoir effects and paleo sea-level in Taiwan during the early-middle Holocene.

In this study, we use ^{14}C dating to obtain the chronology of the oyster shell. Correcting with the tectonic uplift/subduction of Taipei Basin, the sea level variations represented by the studied area have been compared with the global sea level changes. A series of δ^{18}O and δ^{13}C analyses have been conducted on both modern oyster and the ancient giant oyster shells to assess the paleo-seawater temperature. The results of this study will provide significant information regarding sea level alterations and water temperature in the early Holocene.

2. BACKGROUND AND SAMPLE INFORMATION

Taipei Basin is bordered by the Western Foothills to the east and south, the Linkou Tableland to the west, and the Tatun Volcanoes to the north (Figure 1). The area was part of the uplifting orogen formed by the collision between the Luzon Arc and the China continent before middle Quaternary (~800 Ka) but has been sunk with the Ryukyu Arc system as a result of flipping of subduction polarity since late Quaternary (ca. 400 Ka) (Teng et al. 2001). Due to the Shanchiao normal fault on the western boundary, the Basin located on the hanging wall is tilted toward the west and filled with upper Pleistocene and Holocene sediments. Based on large numbers of deep drill cores and radiocarbon dates, the depositional history of the Taipei Basin has been established (e.g., Teng et al. 2001; Chen et al. 2008; Su et al. 2018). The uppermost (youngest) stratum is called Sungshan Formation, covering the deposits over the past 20 kyrs. After the last glacial maximum (LGM), the sea level rose rapidly. Around 10,000 years ago, seawater entered Taipei Basin through Kuandu Passage along Tamsui River, forming a vast inland bay (Chen et al. 2008; Su et al. 2018). With the large amount of sediment input from Xindian Creek, Dahan Creek and Keelung River which are the main branches of Tamsui River drainage system, the inland bay was quickly filled up with muddy sediments, up to 100 m thick in the deepest part of the western side of Taipei Basin and decreasing thickness toward the eastern edge of the basin. After the sea level dropped about 6000 years ago, the Taipei basin was formed predominantly with deposited river sediments. Out of 23 drill cores over the basin, four cores contain marine shells (Su et al. 2018). Among the total 66 ^{14}C dates from the 23 cores, five ^{14}C dates from the four cores on marine shells exited between 20 and 40 m core depths, with age ranges of 10130~8210 cal BP (2σ). The majority of the ^{14}C dates were on plant remains in the drill cores. None of the samples from the previous studies could be used for the identification of marine shoreline deposits.

During construction work in 2002, a stratum containing *Placuna placenta* (Linnaeus, 1758) (hereafter *P. placenta*) shells and oyster reefs was opened in the Taipei metropolitan area (25.03704°N, 121.56774°E) (Figure 1). A *P. placenta* shell was taken from 9.5 m deep below the ground surface and the latter has an elevation of 10 m a.s.l., which means that the *P. placenta* shell sample (TPS-9.5 in Table 1 and red star in the lower left panel of Figure 1) has an

Table 1   The AMS ^{14}C dating results of the giant oyster and LSC ^{14}C dating results of the samples from Taipei Basin. NTU- is the lab code of the LSC Lab (closed in 2014), whereas NTUAMS- is the lab code of the NTUAMS Lab. The calibrated ^{14}C ages of Marine20 and IntCal20 are in 2σ (95%) error. See text for the calculation of weighted average and standard deviation.

Lab code	Sample ID	pMC (%)	^{14}C age (BP)	X_i^{Adj} (year BP)	Marine20 (cal BP)	IntCal20 (cal BP)
NTU-3809 plant	TPS-UA	40.49±0.23	7260±46			**8090±90**
NTU-3810 oyster	TPS-UB	38.28±0.19	**7713±40**	7647±50	**7925±175**	
NTU-3856 shell	TPS-9.5m	38.62±0.26	7543±54	7577±62	7845±175	
NTUAMS-6758	TPS-1	40.50±0.54	7260±106	7194±111	7490±240	
NTUAMS-6759	TPS-2	39.60±0.45	7441±92	7375±96	7660±220	
NTUAMS-6760	TPS-3	39.55±0.46	7452±93	7386±98	7680±225	
NTUAMS-6761	TPS-4	39.40±0.47	7482±95	7416±100	7705±225	
NTUAMS-6762	TPS-5	38.79±0.46	7607±95	7541±99	7805±230	
NTUAMS-6763	TPS-6	39.57±0.45	7447±91	7381±96	7665±215	
NTUAMS-6764	TPS-7	40.06±0.58	7349±117	7283±121	7580±260	
Average and standard deviation of shell AMS dates			**7444±103**		**7660±93**	
NTU-4057 shell	BJ 18.1m	35.41±0.70	8340±159	8274±162	8630±415	
NTU-4102 shell	BJ 22.2m	35.82±0.42	8247±94	8181±99	8510±290	

elevation of 0.5 m a.s.l. at the sampling time. This shell was dated by ^{14}C dating using beta counting method in the Liquid Scintillation Counting (LSC) Lab at National Taiwan University (NTU), yielding a ^{14}C age of 7643±54 BP (NTU-3856 in Table 1). Five meters below this *P. placenta* shell sample, an oyster reef contained many giant oyster shells with the size of 20 to 40 cm long. The largest oyster shell containing both left (lower) and right (upper) valves was collected. Initially, a grass sample existed in the oyster shell. Both the grass sample (TPS-UA in Table 1) and the right valve of the shell (TPS-UB) were dated with LSC ^{14}C method, yielding the conventional ^{14}C ages of 7260±46 and 7713±40 BP, respectively. In 2020, the left valve of the oyster was selected for this study (Figure 2). According to the sampling position, the oyster shell had an elevation of –5 m a.s.l. at the sampling time.

Both *P. placenta* shell and oyster shell existed in a muddy black silt clay layer which is more than 5-m thick. These marine bivalves should live in brackish-to-saline water environment. The samples should be naturally deposited and preserved well. The longest axis of the oyster shell is about 42 cm (Figure 2). In this study, we also used LSC ^{14}C dates of two shell samples from a drill core (Red triangle in Figure 1) located in about 5 km north away from the giant oyster site. These two shells (BJ 18.1 and BJ 22.2 in Table 1) were collected from the depths of 18.1 and 22.2 m in the drill core respectively. The ^{14}C ages of the samples were dated by LSC Lab at NTU.

Besides the ancient oyster shell sample, two modern oyster shells were collected from a cultured oyster pool of Fisheries Research Institute Tainan Branch, Council of Agriculture of Taiwan in Feb. 2008 (Figure 3). These modern oysters were cultured in marine water for a year.
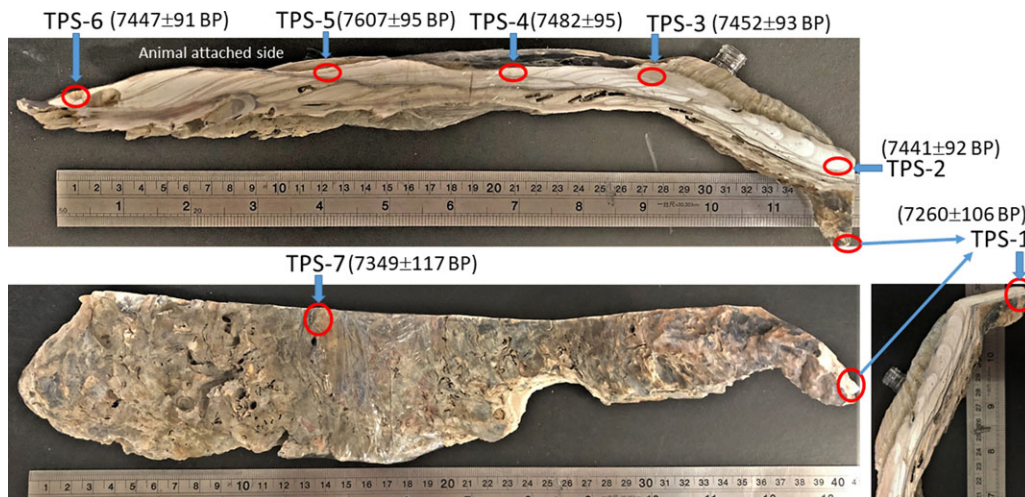
Figure 2　Picture of the giant oyster shell with the conventional ^{14}C ages (not calibrated).

3. METHODS

The giant oyster shell was washed with tap water using a steel brush to remove any detritus from the surface, then cut into half along the growth axis. After drying, seven spots were selected as subsamples for AMS ^{14}C dating using a hand-held dental drill (Figure 2). The oldest part (between TPS-1 and TPS-2) was selected for stable isotope samples. The shell powder was measured by X-ray diffraction (XRD) to determine carbonate minerals.

3.1 AMS ^{14}C Dating

Accelerator mass spectrometry (AMS) ^{14}C dating was performed in the NTUAMS Lab at NTU with a 1.0 MV Tandetron Model 4110 BO AMS. Powdered ~12 mg of each carbonate sample from the oyster were wrapped in a silver cup and placed in a reaction vessel which has a side arm containing 1ml of 100% H_3PO_4. The reaction vessel was placed on a vacuum line. After the vacuum of the reaction vessel reached 10^{-5} mbar, the sample was reacted with the acid to produce CO_2 in the sealed reaction vessel. Then, the collected sample CO_2 was purified and quantified through the vacuum line and transferred into a combination tube containing Fe power in a 6-mm tube and Zn+TiH_2 power in a 9-mm tube (Xu et al. 2007). In our lab, we use Fe:C of 3:1. The sealed combustion tube was placed in a Muffle furnace for graphitization under 550°C. The sample graphite was pressed in a target holder and placed on the AMS for measurement (Zhao et al. 2015). For every batch of the samples, at least three oxalic acid standards (OXII, SRM 4990C), three carbonate backgrounds (NTUB, made from Upper Devonian limestone) and two known-age inter-comparison samples (IRI, distributed by the University of Glasgow) were processed in the same procedures and measured with the sample targets.

Both ^{14}C/^{12}C and ^{13}C/^{12}C ratios measured by the AMS on all graphite targets were used for age calculation described in Li et al. (2022). The AMS measurement was set up for four cycles and each cycle contained 50 blocks (30 seconds for every block). When the ^{14}C counts in a measurement cycle reached 40,000, the counting would stop. Therefore, ^{14}C counts of OXII are normally greater than 40,000, with a statistic error <0.5%. In general, the precision of the ^{14}C
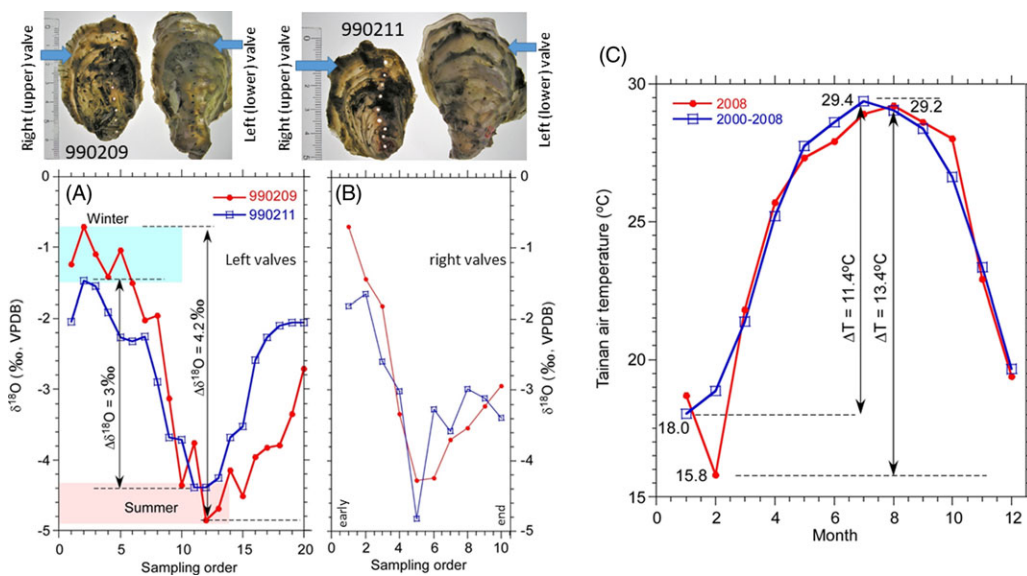
Figure 3   A and B: The $\delta^{18}O$ profiles of two modern oyster shells (990209 and 990211) cultured in the seawater in Tainan. The sampling order reflects the growth time sequence with 0 denoting the earlies time and the maximum denoting collection time. C: The monthly air temperature changes (red line) during 2008 and the monthly average air temperature changes (blue line) during 2000–2008 in Tainan. The modern oyster shell 990211 has $\Delta\delta^{18}O = 3‰$, which reflects a temperature change of 13°C (3/0.232). This agrees with air temperature change of Tainan.

dating at the NTUAMS Lab is better than 3%. All AMS ^{14}C ages were calibrated by using the calibration curves of Marine20 (Heaton et al. 2020) and IntCal20 (Reimer et al. 2020; Stuiver et al. 2018).

3.2 Stable Isotopes

For the modern oyster shells, 20 subsamples on the left valves and 10 subsamples on the right valves of each oysters were taken using a hand-held dental drill with a drill bit of 0.5 mm in diameter (Figure 3). The sample order is from old to young. For the giant ancient oyster shell, a total of 79 subsamples in a 5.5-cm selected section were drilled along the growth axis for $\delta^{18}O$ and $\delta^{13}C$ analyses (Figure 4). About 10 µg of sample powder was wrapped in a tin cup and placed in a Multicarb automatic system (which is an automatic inlet sampler) connected with a Micromass IsoPrime isotope ratio mass spectrometer at the Department of Earth Sciences, National Taiwan Normal University. Each loading set contains 60 samples, with three international standards (NBS-19) in the beginning and one working standard (MAB, a pure marble formed in Taroko National Park of Eastern Taiwan ca. 250 million years ago with $\delta^{18}O = –6.9‰$ and $\delta^{13}C = 3.4‰$) every 7 samples to monitor any instrumental shift. The analytic precisions for $\delta^{18}O$ and $\delta^{13}C$ on standard samples were 0.06‰ and 0.04‰, respectively. All $\delta^{18}O$ and $\delta^{13}C$ values were reported to refer V-PDB at 25°C.

3.3 XRD Analysis

Since the isotopic fractionation between carbonate and its parent water depends on carbonate minerals, i.e., calcite, aragonite and dolomite (Friedman and O'Neil 1977), it is necessary to know the mineral of the oyster shells. X-ray diffraction (XRD) analysis on the ancient and
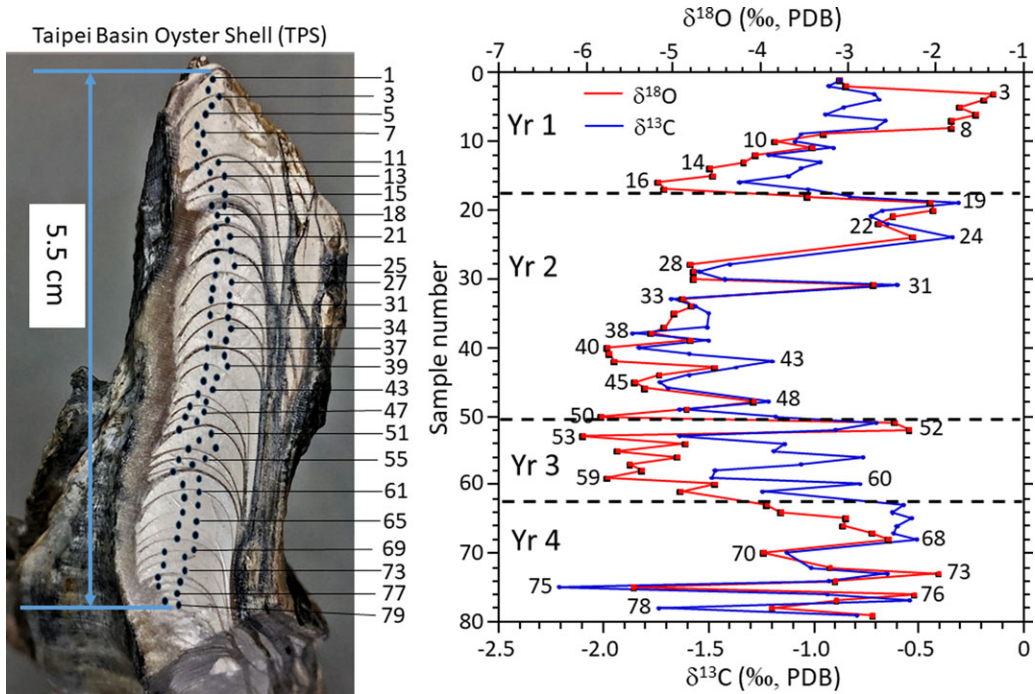
Figure 4   The δ^{18}O (red line) and δ^{13}C (blue line) profiles in a section of the giant oyster reveal 4-yr cycles with lighter values in the summer and heavier values in the winter (confirmed by modern oyster shell measurement).

modern oyster shell samples was carried out using BRUKER binary V3 with Cu target with 30 mA and 40 kV in the Micro-Nano Mineral Lab at National Cheng-Kung University, Taiwan. The results show that the carbonate mineral in all samples is calcite.

4. RESULTS AND DISCUSSIONS

4.1 Chronology

The seven AMS ^{14}C dates (TPS-1 to −7) and other LSC ^{14}C dates are listed in Table 1. First of all, we shall compare the dating results between AMS and LSC methods. TPS-UB is the right valve of the giant oyster shell whereas TPS-1 to −7 samples are from the left valve of the same oyster. They should have the same age. The AMS ^{14}C ages of the shell range from 7260±106 to 7607±95 BP, resulting in a weighted average with standard deviation of 7444±103 BP (n = 7) (Table 1). The calculations of the weighted average and standard deviation are following (Bevington 1969):

$$\text{Weighted average of A} = \mu = \Sigma_i(A_i/\sigma_i^2)/\Sigma_i(1/\sigma_i^2) \tag{1}$$

$$\eta \text{ of A} = \text{Sqrt}[\{(1/(n-1))^*\Sigma_i((A_I - \mu)/\sigma_i)^2]\}/\{(\Sigma_i(1/\sigma_i^2))/n\}] \tag{2}$$

where μ is the weighted average; σ_i is the uncertainty in A_i; η is the standard deviation of A; n is the number of ages in the calculation. Similarly, for ΔR calculation, the weighted average ΔR value and its standard deviation will be used ΔR to replace A in the above equations.

The 347-yr age range of the AMS ages does not show any trends (Figure 2). According to previous investigations, no *C. gigas* could live more than 20 years (e.g., Wang et al. 1995). Therefore, the large AMS ^{14}C age range of the giant oyster might be attributed to laboratory dating uncertainty and/or the natural variation of the marine reservoir effect. The LSC ^{14}C age of the shell is 7713±40 BP which is very close to the oldest AMS ^{14}C age (7607±95 BP) of the shell, but 269 years older than the averaged AMS ^{14}C age (7444±103 BP). Considering the age uncertainties, the LSC ^{14}C age is slightly older than the average AMS ^{14}C age.

Second, we shall compare the age of the organic sample with the ages of the oyster shell. Sample TPS-UA is a grass sample taken from the inside of the oyster shell. This grass sample was dated by LSC, yielding a ^{14}C age of 7260±46 BP (Table 1). This age does not need to make marine reservoir age correction. Using the calibration curve IntCal20 (Reimer et al. 2020), the calibrated ^{14}C age of this grass sample is 8090±90 cal BP. If we compare uncalibrated ^{14}C ages of the grass sample with the LSC dated right valve and the 7 AMS dates of the left valve from the same oyster shell, the grass ^{14}C age (7260±46 BP) is apparently younger than the LSC ^{14}C age (7713±40 BP) and the averaged AMS ^{14}C age (7444±103 BP) of the shell, it is the same as the shell AMS ^{14}C ages of TPS-1 and TPS-7 within uncertainties. In principle, the grass sample would get into the shell either when the oyster was alive or after the oyster was dead. If the grass and oyster had the same depositional age, then the older ^{14}C age of the oyster shell should be caused by the marine reservoir effect. Thus, we should compare the calibrated ^{14}C ages of the grass sample and the shell samples.

Using http://calib.org/marine/, we have found six nearest points (all within 60 km) to the study site. The six ΔR values range from –105±41 to –23±42 years (Yoneda et al. 2007), yielding a weighted average of –66±30 years. Following the equations in Heaton et al. (2020), X_i^{Adj} and σ_i^{Adj} values were calculated (Table 1). These values were used to obtain the calibrated ages by Marine20 calibration curve. The calibrated ages are from 7490±240 to 7805±230 cal BP (2σ), resulting in a weighted age of 7660±96 cal BP (n = 7) (Table 1). Thus, we have three key numbers in comparison: 8090±90 cal BP of the grass sample; 7925±175 cal BP of the LSC dated oyster shell (right valve); and the weighted average (7660±93 cal BP) of the 7 AMS ages from the left valve samples. The comparison indicates that the calibrated ^{14}C ages of both LSC dated grass and oyster shell agree very well. However, the grass age is close to the old AMS ages (e.g., TPS-3 to TPS-5 in Table 1) within uncertainties but younger than the weighted average age of the AMS dates. Since we do not have AMS dating result on the grass sample, the grass age older than the average AMS age of the oyster shell may be caused by the systematic dating difference between the LSC Lab and the AMS Lab. As mentioned earlier, the LSC age is older than the average AMS age of the oyster shell (Table 1). For safe interpretation, we will use the LSC dated grass age and the weighted AMS age of the oyster shell (8090~7660 cal BP) for the period of the ancient shoreline. However, the depositional age of the giant oyster shell (or the oyster reef) should be ~7660 cal BP based on the AMS dating results.

4.2 $\delta^{18}O$ and $\delta^{13}C$

Many marine shells and freshwater carbonates have equilibrium exchange of carbon and oxygen isotopes between carbonate and water (Friedman and O'Neil 1977; Li et al. 2004, 2008; Ravelo and Hillaire-Marcel 2007). The oxygen isotope equilibrium can be described by the following equation (Friedman and O'Neil 1977):

$$T(°C) = 17.0 - 4.52(\delta^{18}O_c - \delta^{18}O_w) + 0.13(\delta^{18}O_c - \delta^{18}O_w)^2 \qquad (3)$$

where $\delta^{18}O_c$ (VPBD) and $\delta^{18}O_w$ (SMOW) are $\delta^{18}O$ values of calcite and equilibrated water, respectively; T is the water temperature at the equilibrium exchange. Eq. (3) can be simplified as the following equation in a temperature range of 0~50°C (Zhao et al. 2015):

$$\delta^{18}O_{calcite} \text{ (VPDB)} - \delta^{18}O_{water} \text{ (SMOW)} = 3.945 - 0.232T(°C) \qquad (4)$$

Although it is difficult to know the information of $\delta^{18}O_w$ in the past, for an assumed water $\delta^{18}O$ in a dry season, one can estimate the seasonal temperature. Using stable carbon and oxygen isotope records, we may reconstruct the water temperature of the oyster lived and other conditions ca. 8000 years ago.

Two oyster shells were collected from a culture oyster pool on February 9 and 11, 2008. The oyster pool was using seawater from coastal Tainan City, Taiwan. Figures 3A and 3B exhibit the $\delta^{18}O$ profiles of both left (lower) and right (upper) valves of the two modern oyster shells: 990209 and 990211. All of the $\delta^{18}O$ profiles reveal heavier values in the winter and lighter values in the summer. In the meantime, the $\delta^{13}C$ profiles are positively correlated with the $\delta^{18}O$ profiles, which means that the shell carbonate is in isotopic equilibrium fraction with its parent water. Paleo-temperature can be reconstructed from such a shell (Mook 1971). Here we take the $\delta^{18}O$ profiles of left valves for discussion as the studied ancient oyster shell is a left valve. The $\Delta\delta^{18}O$ values between winter and summer for 990209 and 990211 are 4.2‰ and 3‰ (Figure 3A), respectively. These results indicate that the oyster shells can have $\Delta\delta^{18}O$ values of 3‰~4‰, being lighter in summer and heavier in winter which agrees well with the temperature influence on the oxygen isotopic fractionation. According to Eq. (4), $\Delta\delta^{18}O$ values of 3‰ and 4‰ represent a temperature change of 13°C (= 3/0.232) and 17°C (= 4/0.232), respectively. For such temperature changes between winter and summer, we can examine them with the air temperature change of Tainan City recorded by the meteorological station. Figure 3C shows the air temperature from January to December in Tainan in 2008 as well as the average during 2000–2008. The ΔT between the winter and summer of Tainan in 2008 is 13.4°C. Assuming the water temperature where the oyster lived reflects closely the monthly air temperature, the $\Delta\delta^{18}O$ values of 3‰~4‰ should represent roughly a temperature change of 13°C. Although this estimation involves a variation of the water $\delta^{18}O$ ($\delta^{18}O_{water}$ in Eq. [4]) due to salinity change, the major influence factor on the $\delta^{18}O_{calcite}$ is water temperature because the culture pool used the seawater without adding any freshwater. This study demonstrates that oxygen isotopic fractionation between the oyster shell and its parent water is under equilibrium, so that Eq. (4) can be used for water temperature calculation.

For the ancient oyster shell, the oldest part was selected for high-resolution stable isotope study. In a 5.5-cm section, a total of 79 subsamples were taken (Figure 4), but only 69 samples had $\delta^{18}O$ and $\delta^{13}C$ results due to sample amount limitation. The $\delta^{18}O$ varies from –6.03‰ to –1.33‰, whereas the $\delta^{13}C$ variation is between –2.21‰ and –0.31‰. These profiles show the following features: (1) the $\delta^{18}O$ and $\delta^{13}C$ values co-vary ($R^2 = 0.6$, n = 69); (2) the $\delta^{18}O$ has long-term variations superimposed on minor fluctuations, which may display seasonal cycles; and (3) the $\Delta\delta^{18}O$ values for the long-term cycles are ~4‰ which is close to the value of the modern oyster shells. Although some growth bands (thin dark lines) appear in the picture of the shell section in Figure 4, these bands are certainly not annual bands, based on the $\delta^{18}O$ and $\delta^{13}C$ profiles. To view the $\delta^{18}O$ and $\delta^{13}C$ profiles, the $\delta^{18}O$ values from samples 3–8 are between –2‰ to –1‰, reflecting the winter values under cold water temperatures. Then, the $\delta^{18}O$

sharply increased and reached a minimum of around –5.2‰ (samples 16–17), representing the summer values under warm and less saline water conditions as the relationship of the water δ^{18}O value and salinity is positively correlated (Dämmer et al. 2020). Thus, one may assume the δ^{18}O trend from sample 1 to 18 accounted for a one-year cycle, so we assign the cycle as Year 1 (Yr 1 in Figure 4). The δ^{13}C trend corresponded positively to the δ^{18}O trend, being heavier values in the winter and lighter values in the summer. Unlike the modern cultured oysters which lived in a pool, the ancient oyster lived in a natural environment where the δ^{13}C could be influenced by the δ^{13}C of surface runoff (Li et al. 2008). The δ^{13}C of total dissolved CO_2 (mainly HCO_3^-) in the marine surface water is around 0‰ (V-PDB) under isotopic equilibrium exchange with the atmospheric CO_2. When organic matter is decomposed, the CO_2 from the organic carbon with lighter δ^{13}C enters the surface water, which makes the δ^{13}C of total dissolved CO_2 to be lighter. In the summertime, higher organic matter decomposition under warm and humid conditions in the surface runoff leads to lighter δ^{13}C than that in the wintertime. In Taiwan, summer monsoon rains have lighter δ^{18}O due to amount and source effects. In contrast, the δ^{18}O and δ^{13}C of surface water in wintertime are relatively heavier. Therefore, the δ^{18}O and δ^{13}C values have covariance. Based on the δ^{18}O and δ^{13}C profiles shown in Figure 4, one may identify four annual cycles. Except Yr 3, the δ^{18}O and δ^{13}C in other three years were strongly correlated. The poor correlation of δ^{18}O and δ^{13}C in Yr 3 was probably due to the influence of heavy and frequent rains in the warm seasons because the δ^{18}O values were quite depleted (Figure 4). Note that the fluctuations of the δ^{18}O and δ^{13}C in the wintertime were relatively small, whereas the summer δ^{18}O and δ^{13}C variations were large, especially when the oyster got older. The large fluctuation in the summer δ^{18}O and δ^{13}C could be attributed to the salinity change because heavy rains (or typhoon) mainly occur in summer to autumn. For such a reason, the winter δ^{18}O value reflects more temperature effect but less salinity effect on isotopic exchange with calcium carbonate and its parent water.

4.3 Sea Level during 8090~7660 cal BP

The ancient oyster lived in a shallow saline water environment (less than 5 m water depth) around ~7660 cal BP based on the AMS dating result. This oyster reef was –5.5 m a.s.l., representing a high stand of the marine transgression in Taipei Basin during the early Holocene. In the same section, the *P. placenta* shell sample which had a LSC ^{14}C age of 7643 ±54 BP and Marine20 curve calibrated ^{14}C age of 7845±175 cal BP was 0.5 m a.s.l. at the sampling time (Table 1 and Figure 1). Thus, according to the LSC dating results of the grass sample, oyster shell and the *P. placenta* shell as well as the AMS dating results, depositional age of the studied stratum was 8090~7660 cal BP. The studied section contained at least 5 m thick sediments between the oyster shell and the *P. placenta* shell. However, the ^{14}C dating results of the oyster shells and *P. placenta* shell are no difference within uncertainties (Table 1). The 5-m thick sediments of the studying site were deposited very fast within a short time period around 8000 cal BP, which is the sedimentary feature of marine transgression. The same situation was found in a drill core which was located ~5 km north of our studying site (Figure 1). Two LSC ^{14}C ages of the marine shell samples from core depths of 18.1 and 22.2 m were 8630±415 and 8510±290 cal BP (2σ), respectively (Table 1). The 4-m thick sediments were also deposited very fast. Thus, the marine transgression in Taipei Basin occurred during 8600 cal BP to 7660 cal BP. One can treat the oyster and *P. placenta* site as a shoreline during 8090~7660 cal BP. Assuming the elevations of these shells represent the sea level in the early Holocene, we can estimate their minimum sea level elevations.

Due to the normal fault of Shanchiao Fault, Taipei Basin has been sinking through the late Pleistocene to Holocene. Based on the ^{14}C dates and sample depths of a drill core (Sungshan No. 2) that is the nearest core from our study site, the tectonic subsidence/uplift rates were 0.0, +0.2 and −0.3 mm/yr at 8780, 9610 and 9790 cal BP, respectively (Chen et al. 2008). Assuming a subsidence rate of 0.1 mm/yr on the eastern edge of Taipei Basin throughout Holocene, the subsidence at the sampling site would be 0.8 m over the past 8300 years, which is within the uncertainty of the estimation. Thus, the oyster had an elevation of –5 m a.s.l. and the *P. placenta* shell had 0 m a.s.l. during 8090~7660 cal BP. Given a range of 1–3 m water depths for the marine animals to live, the elevations of the sea level are estimated 1~3 m a.s.l. during 8090~7660 cal BP. From 8600 cal BP to 7600 cal BP, the sea level was rising; and the sea level was about 1–3 m higher during 8090~7660 cal BP than the modern sea level.

Chen et al. (2008) concluded: (1) seawater entered Taipei Basin around 10,000 cal BP during the Holocene marine transgression which turned the sedimentary environment of Taipei Basin from freshwater lake to semi-saline estuary environments; (2) the sea level stand in Taipei Basin reached the highest level during 8160~7850 cal BP which was higher than modern sea level; (3) then sea level dropped. Our study of the marine shells agrees well with the above conclusions, but further refines the sea level change in the early Holocene: the sea level rose from 8600 cal BP to 7600 cal BP; and the decline of sea level was after 7600 cal BP.

According to the review paper of Smith et al. (2011), sea level rise during the early Holocene behaved differently in different regions. However, the meltwater flux from the discharges of Lake Agassize/Ojibway in North America occurred around 8470 cal BP caused a strong increase in sea level. Our oyster shell was deposited shortly after this time, agreeing well with the sea level rise event. The Melting Water Pulse (MWP) 1d marked between 7100 and 7700 cal BP in Figure 3 of Smith et al. (2011) was supported by the studies of Liu et al. (2004) and Yu et al. (2007). The average AMS dating result of the *oyster* shell in the study site, 7660±96 cal BP (Marine20 calibrated), agrees very well with the age of MWP 1d. Furthermore, many previous studies have shown that sea level rose from 8300 cal BP to 7600 cal BP (Bird et al. 2007, 2010; Li et al. 2012; Smith et al. 2013; Tanabe 2020). This rising trend clearly appeared in our study site. Although some previous publications indicated that the Holocene high stand of sea level reached the maximum between 5000 and 7000 cal BP (e.g., Zong 2004; Bird et al. 2010; Smith et al. 2013; Tanabe 2020), we had no marine shells in our study section to support the above scenario. The marine regression in Taipei Basin might occur as early as 7000 cal BP (Teng et al. 2004; Chen et al. 2008).

In addition, Chen et al. (2020) studied the marine terrace evolution in the Coastal Range of eastern Taiwan. Based on ^{14}C ages and shore features, they concluded that the constructive processes of marine transgression during 14,790~8500 cal BP resulted in a relatively rapid sea-level rise associated with fast shoreline transgression. The sea level reached at the peak of the postglacial marine transgression around 8500 cal BP (Chen et al. 2020). Since 8500 cal BP, the sea level started to fall and five marine terraces formed during the regressional sequences. The highest marine terrace (T1) was dated in an age range of 8150±150~7705 ± 225 cal BP, reflecting the beginning of marine regression earlier than 8150 cal BP. Our dates in Table 1 show (1) the postglacial marine transgression from 8600 cal BP to 7660 cal BP and (2) the sea level reached the peak during 8090~7660 cal BP. Our dating results of the marine transgression and regression agree with the ages of Chen et al. (2020).

4.4 Estimated Winter Temperature around ~7660 cal BP

In Section 4.2 above, we have demonstrated the isotopic equilibrium fractionation between the marine shell and its parent water and identified at least four annual cycles in the shell. These giant oysters were able to live at least four years around ~7660 cal BP. However, such large oysters have not been found in late Holocene in Taiwan. *Crassostrea gigas* is widely distributed in Japan, Korea, China and successfully cultured in the coast water of European countries (e.g., France, Norway, etc.). According to early studies, *Crassostrea gigas* is able to survive in a water body with relatively large ranges of salinity and water temperature (Miossec et al. 2009). The cultured oyster in Taiwan can live in water with salinity as low as 9‰ (Seawater is about 33–35‰). Temperature requirement for *Crassostrea gigas* is above 18°C for spawning (Mann 1979) and above 22°C for larval development (Arakawa 1990; Shatkin et al. 1997). Here we estimate the winter temperature around ~7660 cal BP to illustrate temperature influence on the disappearance of the giant *Crassostrea gigas* in Taiwan.

As we discussed the $\delta^{18}O$ of the shell would have larger influence from the depleted $\delta^{18}O$ of meteorological water in the summer, while the $\delta^{18}O$ value of the winter shell carbonate should have minimal influence of freshwater. If we assume the maximum $\delta^{18}O$ in each year in the oyster shell reflecting isotopic equilibrium under coldest temperature and heaviest $\delta^{18}O$ of water, then we can estimate the winter temperature around ~7660 cal BP.

In Taipei Basin, cold and dry season resulted in the heaviest $\delta^{18}O$ and $\delta^{13}C$ in the oyster shell carbonate. During this season, the $\delta^{18}O$ of coastal water had least influence of surface runoff. Thus, we use the heaviest $\delta^{13}C_c$ in each year to pinpoint the $\delta^{18}O_c$ of cold and dry season. With an assumed $\delta^{18}O$ of water, we can calculate the water temperature. From Figure 4, the maximum $\delta^{18}O$ value in each year are selected as below. Using Eq. (4) and assuming $\delta^{18}O_w = –1.7‰$ to $–1.2‰$ (SMOW), we can calculate winter temperature:

Yr 1, Sample 3, $\delta^{13}C = –0.71‰$, $\delta^{18}O_c = –1.33‰$, T = 15.3°C to 17.6°C
Yr 2, Sample 20, $\delta^{13}C = –0.68‰$, $\delta^{18}O_c = –2.02‰$, T = 18.5°C to 20.8°C
Yr 3, Sample 52, $\delta^{13}C = –0.89‰$, $\delta^{18}O_c = –2.30‰$, T = 19.8°C to 22.1°C
Yr 4, Sample 68, $\delta^{13}C = –0.51‰$, $\delta^{18}O_c = –2.54‰$, T = 20.9°C to 23.3°C

Considering the modern sea surface water has a $\delta^{18}O_w$ of 0‰, the $\delta^{18}O_w$ range of $–1.7‰$ to $–1.2‰$ for the oyster depositional site with minimal freshwater influence should be reasonable. First of all, the $\delta^{18}O_w$ value of the modern seawater is for open ocean surface water. In general, coastal water has lower salinity due to influence of surface runoff, so that $\delta^{18}O_w$ value of coastal water should be lighter than that of the open ocean surface water. Second, the studied site represents a higher sea level shoreline, which means that the seawater rose due to more freshwater input. Thirdly, many studies show that the climatic conditions were generally warmer and wetter during the early-to-middle Holocene in Taiwan and south China (e.g., Ding et al. 2020). For wetter climates and higher sea level in the coastal environment, lower salinity and lighter $\delta^{18}O_w$ value are expected. Therefore, the $\delta^{18}O_w$ value of the studied site should be lighter than 0‰. For these reasons, we assume that the $\delta^{18}O_w$ was $–1.7‰$ to $–1.2‰$. The calculated winter temperature ranged from 15 to 23°C. The large shift in winter temperature during the four years may be due to salinity influence on the calculation. The estimated winter temperature around ~7660 cal BP was warmer than the modern winter temperature in Taipei which is 14–16°C. The giant oyster lived in ~7660 cal BP under a warmer condition. Then, the disappearance of the oyster in the late Holocene in Taiwan should not be due to current global warming.

5. CONCLUSIONS

A giant (42-cm long) oyster (*Crassostrea gigas*) shell from eastern edge of Taipei Basin has been dated by AMS ^{14}C method, resulting in a weighted average of 7444±103 BP (n = 7) which is close to the LSC ^{14}C age (7260±46 BP) of a grass from the oyster shell. Based on the calibrated LSC ^{14}C ages of the grass (8090±90 cal BP) and the oyster shell (7925±175 cal BP) and the weighted calibrated age of the 7 AMS ages (7660±96 cal BP), a depositional age of the >5-m thick shoreline sediments during 8090~7660 cal BP is obtained. The ^{14}C ages of the marine shells in the studying sites of Taipei Basin indicate that sea-level rose from 8600 cal BP to 7600 cal BP, reached an elevation about 1~3 m higher than the modern sea level during 8090~7660 cal BP. No evidence from the study site support the maximum highstand between 5000 and 7000 cal BP.

The high-resolution δ^{18}O and δ^{13}C profiles of the oldest 5.5-cm section in the giant oyster shell appeared four annual cycles. Based on the δ^{18}O values, the winter temperature in Taipei Basin around ~7660 cal BP was estimated as 15~23ºC, warmer than today. The disappearance of this type of oyster in Taiwan during the late Holocene should not be due to a warming trend.

ACKNOWLEDGMENTS

REFERENCES

Alves EQ, Macario K, Ascough P, Bronk Ramsey C. 2018. The worldwide marine radiocarbon reservoir effect: definitions, mechanisms, and prospects. Reviews of Geophysics 56(1):278–305.

Arakawa KY. 1990. Natural spat collecting in the Pacific oyster *Crassostrea gigas* (Thunberg). Marine Behaviour and Physiology 17:95–128.

Bevington PR. 1969. Data reduction and error analysis for the physical sciences. New York: McGraw-Hill.

Bird MI, Fifield LK, Teh TS, Chang CH, Shirlaw N, Lambeck K. 2007. An inflection in the rate of early mid-Holocene eustatic sea-level rise: a new sealevel curve from Singapore. Estuarine. Coastal and Shelf Science 71:523–536.

Bird MI, Austin WEN, Murster CM, Fifield LK, Mojtahid M, Sargeant C. 2010. Punctuated eustatic sea-level rise in the early mid-Holocene. Geology 38:803–806.

Chen W-S, Lin C-C, Yang C-C, Fei L-Y, Shea K-S, Kung H-M, Lin P-Y, Yang H-C. 2008. The temporal and spatial evolution of sedimentary sequence framework and tectonics of the Taipei Basin since the Late-Pleistocene. Bulletin of the Central Geological Survey 21:61–106. In Chinese with English abstract.

Chen W-S, Yang CY, Chen ST, Huang YC. 2020. New insights into Holocene marine terrace development caused by seismic and aseismic faulting in the Coastal Range, eastern Taiwan. Quaternary Science Reviews 240:106369.

Dämmer LK, Nooijer LD, Sebille EV, Haak JG, Reichart G-J. 2020. Evaluation of oxygen isotopes and trace elements in planktonic foraminifera from the Mediterranean Sea as recorders of seawater oxygen isotopes and salinity. Climate of the Past 16:2401–2414.

Ding XD, Zheng LW, Zheng XF, Kao S-J. 2020. Holocene East Asian summer monsoon rainfall variability in Taiwan. Front. Earth Sci. 8:234. doi: 10.3389/feart.2020.00234

Escapa M, Isacch JP, Daleo P, Alberti J, Iribarne O, Borges M, Dos Santos EP, Gagliadini DA, Lasta M. 2004. The distribution and ecological effects of the introduced Pacific oyster *Crassostrea gigas* (Thinberg, 1793) in northern Patagonia. Journal of Shellfish Research 23(3).

Friedman I, O'Neil JR. 1977. Compilation of stable isotope fractionation factors of geochemical interest. US Geological Survey Professional Paper, P-0440-KK. p. 1–12.

Hadden CS, Hutchinson I, Martindale A. 2023. Dating marine shell: a guide for the wary North American archaeologist. American Antiquity 88(1):62–78.

Heaton TJ, Köhler P, Butzin M, Bard E, Reimer RW, Austin WEN, Bronk Ramsey C, Grootes PM,

Hughen KA, Kromer B, Reimer PJ, Adkins J, Burke A, Cook MS, Olsen J, Skinner LC. 2020. Marine20—the marine radiocarbon age calibration curve (0–55,000 Cal BP). Radiocarbon 62:779–820. doi: 10.1017/RDC.2020.68

Li H-C, Bischoff JL, Ku T-L, Zhu Z-Y. 2004. Climate and hydrology of the Last Interglaciation (MIS 5) in Owens Basin, California: isotopic and geochemical evidence from core OL-92. Quaternary Science Reviews 23:49–63.

Li H-C, Chang Y, Berelson WM, Zhao M, Misra S and Shen T-T. 2022. Interannual variations of $D^{14}C_{TOC}$ and elemental contents in the laminated sediments of the Santa Barbara Basin during the past 200 years. Front. Mar. Sci. 9:823793. doi: 10.3389/fmars.2022.823793

Li H-C, Xu X-M, Ku T-L, You C-F, Buchheim HP, Peters R. 2008. Isotopic and geochemical evidence of palaeoclimate changes in Salton Basin, California, during the past 20 kyr: 1. $\delta^{18}O$ and $\delta^{13}C$ records in lake tufa deposits. Palaeogeography, Palaeoclimatology, Palaeoecology 259:182–197.

Li Y-X, Törnqvist TE, Nevitt JM, Kohl B. 2012. Synchronizing a sea-level jump, final Lake Agassiz drainage, and abrupt cooling 8200 years ago. Earth and Planetary Science Letters 315–316:41–50

Liew PM, Huang CY, Tseng MH. 1997. Preliminary Study on the Late Quaternary climatic environment of the Taipei Basin and its possible relation to basin sediments. J. Geol. Soc. China 40(1):17–30.

Liu JP, Milliman JD, Gao S, Cheng P, 2004. Holocene development of the Yellow River's subaqueous delta, North Yellow Sea. Marine Geology 209:45–67.

Mann R. 1979. Some biochemical and physiological aspect of growth and gametogenesis in Crassostrea gigas and Ostrea edulis grown at sustained elevated temperatures. Journal of marine biological association of United Kingdom 59:95–110.

Miossec L, Deuff RL, Goulletquer P. 2009. Alien species alert: *Crassostrea gigas* (Pacific oyster). ICES Cooperative Research Report No. 299. 42 p.

Mook WG. 1971. Paleotemperatures and chlorinities from stable carbon and oxygen isotopes in shell carbonate. Palaeogeography, Palaeoclimatol., Palaeoecol. 9:245–263.

O'Connor S, Ulm S, Fallon SJ, Barham A, Loch I. 2010. Pre-bomb marine reservoir variability in the Kimberley region, Western Australia. Radiocarbon 52(3):1158–1165.

Ravelo AC, Hillaire-Marcel C. 2007. Chapter eighteen: the use of oxygen and carbon isotopes of foraminifera in paleoceanography. In: C. Hillaire-Marcel, A. De Vernal, editors. Proxies in Late Cenozoic paleoceanography, developments in marine geology series, vol. 1. Amsterdam: Elsevier. p. 735–764.

Reimer PJ, Austin WEN, Bard E, Bayliss A, Blackwell PG, Ramsey CB, Butzin M, Cheng H, Edwards RL, Friedrich M, et al. 2020. The IntCal20 Northern Hemisphere radiocarbon age calibration curve (0–55 cal kBP). Radiocarbon 62(4):725–757. doi: 10.1017/RDC.2020.41

Shatkin G, Shumway SE, Hawes R. 1997. Considerations regarding the possible introduction of the Pacific oyster (*Crassostrea gigas*) to the Gulf of Maine: a review of global experience. J. Shellfish Res. 16:463–477.

Smith DE, Harrison S, Firth CR, Jordan JT. 2011. The early Holocene sea level rise. Quaternary Science Reviews 30:1846–1860.

Smith DE, Harrison S, Jordan JT. 2013. Sea level rise and submarine mass failures on open continental Margins. Quaternary Science Reviews 82:93–103.

Stuiver M, Reimer PJ, Reimer RW. 2018. CALIB 7.1 [WWW program] available at http://calib.org.

Su PJ, Chi TC, Su TW, Teng LS. 2018. Facies characteristics and depositional history of the Sungshan Formation, Taipei Basin. Western Pacific Earth Sciences 15–18:19–52.

Tanabe S. 2020. Stepwise accelerations in the rate of sea-level rise in the area north of Tokyo Bay during the Early Holocene. Quaternary Science Reviews 248:106575.

Teng LS, Lee CT, Peng CH, Chen WF, Chu CJ. 2001. Origin and geological evolution of the Taipei Basin, Northern Taiwan. Western Pacific Earth Sciences 1(2):115–142.

Teng LS, Lee CT, Liew PM, Sheng-Rong Song, Shuh-Jong Tsao, Huan-Chi Liu, Chih-Hsiung Peng, 2004. On the Taipei Dammed Lake. Journal of Geographical Science 36:77–100.

Teng LS, Yuan PB, Yu NT, Peng CH. 2000. Sequence stratigraphy of the Taipei Basin deposits: a preliminary study. J. Geol. Soc. China 43(3): 497–520.

Wang H, Keppens E, Nielsen P, van Riet A. 1995. Oxygen and carbon isotope study of the Holocene oyster reefs and paleoenvironmental reconstruction on the northwest coast of Bohai Bay, China. Marine Geology 124:289–302.

Xu X, Trumbore SE, Zheng S, Southon JR, McDuffee KE, Luttgen M, Liu JC. 2007. Modifying a sealed tube zinc reduction method for preparation of AMS graphite targets: reducing background and attaining high precision. Nucl. Instrum. Methods Phys. Res. B. 259(1):320–329.

Yang RJ, Wang SL, Burr GS, Liu JT, Fan D. 2019. Holocene variation of radiocarbon reservoir age offshore western Taiwan, derived from paired charcoals and mollusks. Quaternary International 527:79–86.

Yoneda M, Uno H, Shibata Y, Suzuki R, Kumamoto, Kunio Y, Yoshida K, Sasaki T, Suzuki A, Kawahata H. 2007. Radiocarbon marine reservoir ages in the western Pacific estimated by pre-bomb molluscan shells.

Nuclear Instruments and Methods in Physics Research B 259:432–437.

Yu S-Y, Berglund BE, Sandgren P, Lambeck K. 2007. Evidence for a rapid sealevel rise 7600 yr. ago. Geology 35:891–894.

Zhao M, Li H-C, Liu Z-H, Mii H-S, Sun H-S, Shen C-C. 2015. Changes in climate and vegetation of central Guizhou in Southwest China since the last glacial reflected by stalagmite records from Yelang Cave. J. Asian Earth Sci. 114:549–561. doi: 10.1016/j.jseaes.2015.07.021

Zong YQ. 2004. Mid-Holocene sea-level highstand along the southeast coast of China. Quaternary International 117:55–67.